VALIDATION OF DERIVED EQUATION USING ENERGY TECHNIQUE FOR CALCULATING THE CRITICAL BUCKLING LOAD FOR INTERMEDIATE AND LONG COLUMNS

Ahmed Naif Al-Khazaraji [1], Samir Ali Al-Rabii [2], * Hameed Shamkhi Al-Khazaali [3]

1) Assist Prof., Department of Mechanical Engineering, University of Technology, Baghdad, Iraq.
2) Assist Prof., Department of Mechanical Engineering, University of Technology, Baghdad, Iraq.
3) Assist Lect., Department of Machines and Equipment, Institute of Technology, Middle Technical University, Baghdad, Iraq.

Abstract: A new equation has been derived using energy technique (dummy load method) to describe the buckling behavior of intermediate and long columns under dynamic buckling loads compression load and under dynamic combined load with consider of the initial imperfections of the columns and the effect of eccentricity. The results of this equation are compared with the experimentally results of 40 specimens of AISI 303 stainless steel intermediate and long columns tested under dynamic compression loading (compression and torsion) and under dynamic combined loading (compression, bending, and torsion) by using a rotating buckling test machine, and it be found that the derived equation may be used to predict of the theoretical critical buckling load (P_{cr}) under both dynamic compression and combined load with maximum percentage error is 19.3% and 16.8%, respectively.

Keywords: *Energy technique, buckling load, columns, dummy load method.*

اثبات صحة معادلة مشتقة باستخدام تقنية الطاقة لحساب حمل الانبعاج الحرج للاعمدة المتوسطة الطول و الطويلة

الخلاصة: تم في هذا البحث اشتقاق معادلة لوصف سلوك الانبعاج الديناميكي للاعمدة المتوسطة الطول والطويلة تحت تأثير حمل الانضغاط الديناميكي والحمل الديناميكي المركب بأستخدام تقنية الطاقة مع الاخذ بنظر الاعتبار تأثير كل من الانحراف الاولي للعمود وتأثير اللامحورية في تسليط حمل الانضغاط. النتائج النظرية لحمل الانبعاج الحرج من هذه المعادلة تم مقارنتها مع النتائج العملية لحمل الانبعاج الحرج والتي تم الحصول عليها بفحص ٤٠ عينة من اعمدة الصلب المقاوم للصدأ AISI 303 الطويلة والمتوسطة الطول وتحت تأثيركل من حمل الانضغاط الديناميكي (حمل ضغط محوري زائد حمل التواء) والحمل الديناميكي المركب (حمل ضغط محوري وحمل انحناء زائد حمل التواء)، حيث وجد ان المعادلة المشتقة يمكن ان تستخدم للتنبؤ بمقدار حمل الانبعاج النظري للاعمدة تحت تأثير حمل الانضغاط الديناميكي والحمل الديناميكي المركب وبأعلى نسبة مئوية للخطأ ١٩,٣ % و ١٦,٨ % على التوالي.

1. Introduction

A columns are generally categorized into two groups: long and intermediate; sometimes the short compression block is considered to be a third group. The distinction between the three is determined by their behavior. Long columns fail by

---

*Corresponding Author hameedshamkhi@yahoo.com

buckling or excessive lateral bending; intermediate columns, by a combination of crushing and buckling; and short compression blocks, by crushing [1]. The phenomenon of buckling is not limited to columns. Buckling can occur in beams, plates, shells, and other structural members under a variety of loading conditions [2, 3]. Above the elastic limit of a material the modulus of elasticity becomes a function of the stress. In other word, one should know the operating level of the stress before one can find out the modulus. This makes the analysis in the inelastic region complicated [4]. In case of columns with intermediate slenderness, i.e., columns which are stable for stresses higher than the proportionality limit, the failure of intermediate columns occurs subsequent to the onset of inelastic behavior [5]. The main causes of bending in the columns are lack of straightness in member, i.e., initial curvature in the member, eccentricity of the load and non-homogeneity in the material of the column. Every column will have at least small degree of eccentricity [6]. Many aircraft structural component, structural connections between of boosters for space vehicles, certain members in bridge trusses, and structural frameworks of buildings are common examples of columns. Linkage in oscillating or reciprocating machines may also fail by buckling [7, 8]. Quite often the buckling of a column can lead to a sudden and catastrophic failure of a structure or mechanism, and has a result, special attention must be given to the design of columns so that they can safely support their intended loadings without buckling [9]. The buckling of solid and hollow CK35 and CK45 alloy steel columns under dynamic compression, bending, and combined loading of them has been studied theoretically and experimentally. A mathematical model has been derived in order to model the column buckling problem and determine the number of cycles to failure for short, intermediate, and long columns subjected to single and combined loads [10]. A series of experimentally tests on cold formed austenitic stainless steel square, rectangular, and circular hollow section members to examine the buckling behavior of columns and beams under effect of gradually increased single and combined loads (compression, bending, and compression-bending) with two types of ends conditions pin-ends and fixed-ends [11]. A formula has been suggested for beam-column interaction using second order in-plane elastic theory analysis. This theoretical formula was derived to cover, with maximum continuities, the beam column cross-section classes, stability resistance, and pure elastic and pure plastic behavior [12]. The elastic buckling behavior of a cantilever straight I-column subjected to various loads was described by using derived differential equations that based on Yang and Kuos nonlinear virtual work equation for a 3D straight solid beam. The total potential energy and virtual work were expressed and then utilized the variation principle to derive the buckling differential equations for an I-column element [13]. A unified formula for solid and hollow columns has been derived, on the basis of the theory of elasticity, to predict the behavior of circular concrete-filled steel tube under axial compression load. Analytical solution was used to develop unified formula and linear superposition method was used to deal with the problem of the elastic stability of the composite columns [14]. The buckling behavior of columns, including the combined effects of shear force and bending deformations and semi-rigid connections on the elastic critical buckling loads, has been studied by using three different approaches Engesser,

Haringx, and Euler. Classic column cases (i.e. hinged-hinged column, clamped-clamped column, clamped-free column, and clamped-hinged column) were investigated using a "simplifies form" of derived equations depending on boundary conditions of column ends [15].

This paper would like to validate a new derived equation, on the basis of the energy technique, to describe the dynamic buckling behavior and to predict the critical buckling load of intermediate and long columns, including the effects of initial imperfections and eccentricity, by comparing the results, from this derived equation with experimental results of series of stainless steel (AISI 303) circular cross-section columns, of different slenderness ratios, subjected to dynamic compression loading (compression-torsion) and dynamic combined loading (compression-bending-torsion).

2. Theory and Mathematical Model

2.1. *Energy Technique in Deflection analysis*

Many practical engineering problem involve the combination of a large system of simple elements in a complex and often highly statically indeterminate structure [16]. As an alternative to the methods based on differential equations, the analysis of stress and deformation can be accomplished through the use of energy methods. The latter are predicated on the fact that the equations governing a given stress or strain configuration are derivable from consideration of the minimization of energy associated with deformation, stress, or deformation and stress. Application of energy techniques are quite powerful in situations involving a variety of shapes and variable cross sections and a complex problems involving elastic stability and multielement structures [5]. Castigliano's second theorem (Castigliano's method) provides a simple and straightforward approach to the deflection analysis of a complex collection of many engineering problems involve linear load-deflection relations where the forms of the strain energy are known. This theorem state that: when an elastic body subjected to applied forces and reactions, the partial derivative of the strain energy with respect to an applied force $N_i (i = 1, 2, 3, ..., n)$ is equal to the component of displacement at the point of the force that is in the direction of the force (δ_i). Thus

$$\delta_i = \frac{\partial U}{\partial N_i} \qquad (1)$$

In applying Castigliano's theorem, the strain energy (U) must be expressed as a function of the load [5]. When it is necessary to determine the deflection at a point at which no load acts, a dummy load is introduced at the required point in the direction of the desired displacement. The displacement is then found by Castigliano's theorem, equating the dummy load to zero in the final result [5, 17].
The expression for the strain energy (U) in a straight or curved slender bar subjected to a number of common loads (axial force P, bending moment M_z, shearing force V, and torque M_t) is given by [5]

$$U = \int \frac{P^2 dx}{2EA} + \int \frac{M_z^2 dx}{2EI_z} + \int \frac{\alpha V^2 dx}{2AG} + \int \frac{M_t^2 dx}{2JG} \qquad (2)$$

The displacement at any point in the bar then radially be found by applying Castigliano's theorem. Inasmuch as the force P_i is not a function of x, the differentiation of U with respect to P_i under the integral. In so doing, the displacement is obtained in the following convenient form:

$$\delta_i = \int \frac{1}{EA} P \frac{\partial P}{\partial N_i} dx + \int \frac{1}{EI_z} M_z \frac{\partial M_z}{\partial N_i} dx + \int \frac{\alpha}{AG} V \frac{\partial V}{\partial N_i} dx + \int \frac{1}{JG} M_t \frac{\partial M_t}{\partial N_i} dx \qquad (3)$$

In which the integration are carried out over the length of the bar.

2.2. Mathematical model for dynamic buckling

Fig. 1 represents a schematic diagram of a horizontal slender column with fixed-pinned ends and constant cross section subjected to a compression axial load (P), a bending load (F), and a torsional twisting moment (M_t) with constant rotating speed. This schematic diagram represents one of the real cases of loading used in the present research to examine the dynamic buckling behavior under combined loading conditions.
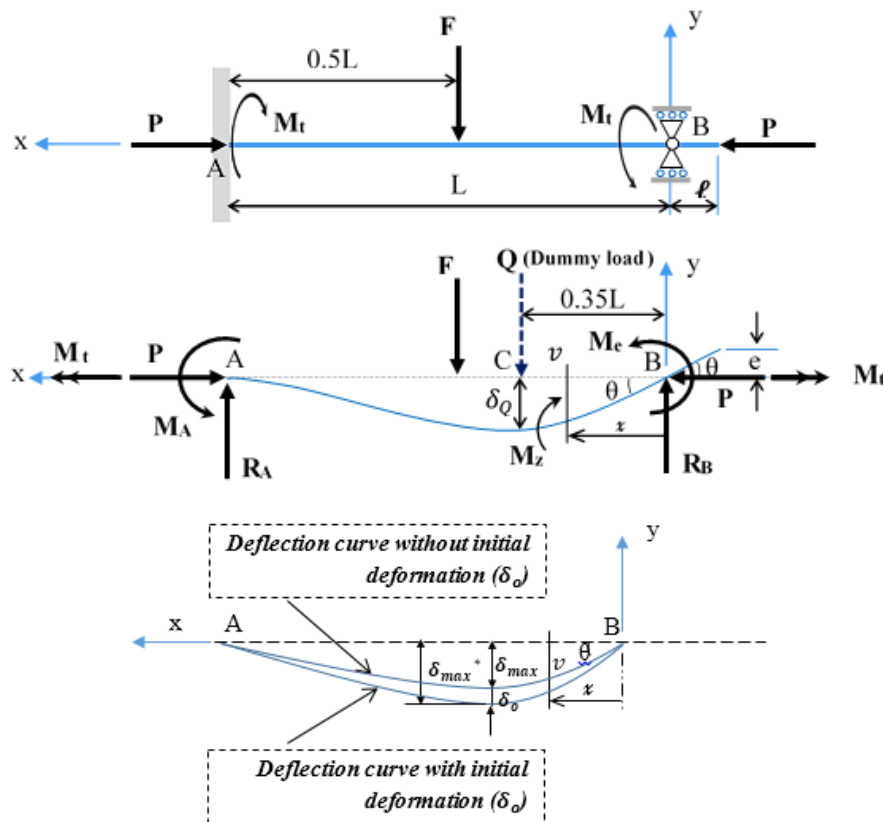

Figure 1. A slender column with fixed-pinned ends conditions under effect of combined loading (a gradually increased axial compression load P, a gradually increased bending load F, and a constant torsional twisting moment M_t.

The mathematical model is based on the assumption that:
1. The material of the column is homogeneous and isotropic.
2. The dimensions of the cross section of the column are exact and the cross section is constant.
3. The applied loads and/or support connections are perfectly positioned geometrically.
4. The axial load and bending load are applied gradually with constant speed of rotation (constant torque).
5. Plane surfaces remain plane after bending.
6. No initial stresses exist from manufacturing assembly operation or residual stresses due to material forming.
7. The contribution of the shear force (V) to the displacement is negligible.

Equation (3) will be abbreviated to

$$\delta_i = \frac{1}{EA}\int_0^L P\frac{\partial P}{\partial N_i}\,dx + \frac{1}{EI_z}\int_0^L M_z\frac{\partial M_z}{\partial N_i}\,dx + \frac{1}{JG}\int_0^L M_t\frac{\partial M_t}{\partial N_i}\,dx \qquad (4)$$

To determine the deflection at a distance 0.35L from point B, a dummy load Q is introduced at point C.

$$\therefore\ \delta_i = \delta_Q,\ N_i = Q, \frac{\partial P}{\partial N_i} = \frac{\partial P}{\partial Q} = 0,\ \text{and}\ \frac{\partial M_t}{\partial N_i} = \frac{\partial M_t}{\partial Q} = 0,$$

Equation (4) will be abbreviated to

$$\delta_Q = \frac{1}{EI_z}\int_0^L M_z\frac{\partial M_z}{\partial Q}\,dx \qquad (5)$$

$\therefore$ Bending moment at any section x from the right-hand side is given by

$$M_z = \begin{cases} -Pv - R_Bx - M_e + M_tv' & (0 \le x \le 0.35L) \\ -Pv - R_Bx - M_e + M_tv' + Q(x - 0.35L) & (0.35 \le x \le 0.5L) \\ -Pv - R_Bx - M_e + M_tv' + Q(x - 0.35L) + F(x - 0.5L) & (0.5 \le x \le L) \end{cases} \qquad (6)$$

Were M_tv' represent the contribution of the torsional loading or twisting moment (M_t) in the bending moment about z-axis (M_z) and this based on the deriving of Greenhill relation [17].

For fixed-pinned ends conditions, and by using superposition method one can write

$$R_B = (0.4964375)Q + \left(\frac{5}{16}\right)F - \frac{M_e}{L} \qquad (7)$$

Substitute (7) in (6) and by taking a partial differentiate of M_z with respect to the dummy load Q and then equating the dummy load to zero(put $Q = 0$) , one can write

$$\frac{\partial M_z}{\partial Q} = \begin{cases} -0.496375\,x & (0 \le x \le 0.35L) \\ -0.496375\,x + (x - 0.35L) & (0.35 \le x \le 0.5L) \\ -0.496375\,x + (x - 0.35L) & (0.5 \le x \le L) \end{cases} \qquad (8)$$

Substitute (6), (7) and (8) in (5) and equating the dummy load to zero, (5) will be as follows:

$$\delta_Q = \frac{1}{EI_z}\left[\int_0^{0.35L}\left(-Pv - \left(\left(\tfrac{5}{16}\right)F - \tfrac{M_e}{L}\right)x - M_e + M_t v'\right)*(-0.496375\,x)dx + \right.$$

$$\int_{0.35L}^{0.5L}\left(-Pv - \left(\left(\tfrac{5}{16}\right)F - \tfrac{M_e}{L}\right)x - M_e + M_t v'\right)*(-0.496375\,x + (x -$$

$$0.35L))dx + \int_{0.5}^{L}\left(-Pv - \left(\left(\tfrac{5}{16}\right)F - \tfrac{M_e}{L}\right)x - M_e + M_t v' + F(x-0.5L)\right) \quad *(-$$

$$\left.0.496375\,x + (x - 0.35L))dx\right] \tag{9}$$

The deflection curve of a column with fixed-pinned ends conditions loaded by an axial load can be represented by the following relation [16]

$$v = 0.715\delta_{max}\left(1 - \cos(a\tfrac{x'}{L}) + \tfrac{1}{a}\sin(a\tfrac{x'}{L}) - \tfrac{x'}{L}\right) \tag{10}$$

Were $a = constant = 4.493$ and δ_{max} =maximum deflection.
For the present research and to simplify the integration, the deflection curve v to be calculated from the right hand of the column as follow:

$$v = -0.715\delta_{max}\left(1 - \cos(a\tfrac{(L-x)}{L}) + \tfrac{1}{a}\sin(a\tfrac{(L-x)}{L}) - \tfrac{(L-x)}{L}\right) \tag{11}$$

$\therefore$ The slope will be, $v' = \frac{0.715\delta_{max}}{L}\left(a\sin(a\tfrac{(L-x)}{L}) + \cos(a\tfrac{(L-x)}{L}) - 1\right)$ (12)

It should be noted, for the present research, the point of applying a dummy load (point C) as shown in Fig. 1, has been selected for two reason: first, for a column with fixed-pinned ends support it known that the an equivalent unsupported length can be calculated by using effective-length factor $K= 0.7$ which give a value of equivalent unsupported length=0.7L measured from point B (Fig. 1). Therefore, the maximum deflection of the column will be at a distance (0.7/2)L=0.35L.Second, from the equation of the deflection curve of a column with fixed-pinned ends conditions (10) or (11), it can be find that the point of maximum deflection $v = 0.999738\,\delta_{max}$ is locate at distance 0.4L from point B, and at this point the slope $v' = 0$ and this will give trivial solution. So, in order to satisfy the two conditions mentioned above, the location of a point C is selected to be 0.35L from point B and this location will give $v = 0.983\,\delta_{max}$.

The moment (M_e) represented an eccentricity moment due to eccentricity distance (e). This moment is given by
$M_e = Pe = P\boldsymbol{\ell}\,\tan\theta$, and for small value of θ, $\tan\theta \cong \theta$ thus,

$$M_e = P\boldsymbol{\ell}\theta = P\boldsymbol{\ell}*(v')_{x=0} \tag{13}$$

Where, θ =slope=$(v')_{x=0}$

From (12) and for $x = 0$, $(v')_{x=0} = \frac{0.715\delta_{max}}{L} * (-5.602938819)$ and by substituting this value into (13) one can write

$$M_e = \frac{0.715\delta_{max}}{L} P\ell * (-5.602938819) \tag{14}$$

By Substituting (11), (12), and (14) into (9) and integration yields

$$\delta_Q = \frac{L}{EI_z}[(0.715\delta_{max} P(-0.06805589 L - 0.2071336 \ell)) + (0.715\delta_{max} M_t(0.1018409)) - (8.704427 * 10^{-3}FL^2)] \tag{15}$$

Now (15) can be arranged to determine the axial compression load P (critical buckling load) as follows:

∴Critical buckling load

$$P_{cr} = \frac{\delta_Q EI}{0.715\delta_{max} HL} - \frac{0.1018M_t}{H} + \frac{8.704427 * 10^{-3}FL^2}{0.715\delta_{max} H} \tag{16}$$

Where, H is a variable and given by $H = -(0.068054 L + 0.2071336 \ell)$

In order to make (16) more accurate, an initial deformation of the column (δ_o) must be considered and to do this, the initial deformation of the column must be subtracted from the displacement at reference point (0.35L from point B) or the displacement under the dummy load (δ_Q) and this means that the strain energy due to real displacement is considered. Thus, one can write (see Fig. 1)

$$\delta_Q{}^* = \delta_Q - \delta_o$$
$$\delta_{max}{}^* = \delta_{max} + |\delta_o| \tag{17}$$

Where, $\delta_Q = \delta_{cr}$ (critical deflection of the column).
And from (11) and by substituting $v = \delta_Q$ and $x = 0.35L$ this will give

$$\delta_{max} = \frac{-\delta_Q}{0.98274} \tag{18}$$

So, the final form of (16) will be
∴Critical buckling load

$$P_{cr} = \frac{(\delta_Q{}^*)EI}{0.715(\delta_{max}{}^*)HL} - \frac{0.1018M_t}{H} + \frac{8.704427 \times 10^{-3}FL^2}{0.715(\delta_{max}{}^*) H} \tag{19}$$

Equation (19) will be used to determine the theoretical critical buckling load throughout the present research. For dynamic compression loading, (19) may be used by setting the bending load equal to zero (F=0). It must be noted that when the column type is intermediate, the Young modulus must be replaced by Tangential modulus (E_t) that calculated from the experimental results of the tensile test of AISI 303 stainless

steel tensile specimens. In order to determine where as the column long or intermediate, effective and critical slenderness ratios are used. The value of the effective slenderness ratio (λ_e) is calculated by using the relation [9]:

$$\lambda_e = \frac{KL}{r} = \frac{L_e}{r} \tag{20}$$

The value of slenderness ratio above which column's type is long and under this intermediate is obtained using the following relation [18]:

$$\lambda_c = \lambda_e = \pi.\sqrt{\frac{E}{\sigma_{pl}}} \tag{21}$$

and by substitution the value of E, σ_{pl} from Table 2, and the value of K=0.7 (for fixed-pinned ends) in (21), the value of critical slenderness ratio is found as $\lambda_c = 86.5$.

In (16) and (19), the effect of a bending load (F) and a twisting load (M_t) on the value of critical buckling load (P_{cr}) has been insulated in two clear mathematical expressions by using energy technique. So, the correct value of theoretical critical buckling load can be predicted. Also, if the position of the point of applying dummy load (Q) has been change, then the limits of integration will be change in (9) and this will give, as a result, different values of critical buckling loads from (19) and only the minimum value of them represents the real value of the critical buckling load of the column.

It should be noted that the direction of applied of the twisting moment M_t (i.e. clockwise or anti-clockwise) will change (15) and/or (19). For example, if one has used an anti-clockwise twisting moment instead of clockwise twisting moment, then the ahead sign of the part that represents the effect of the twisting moment will be changing from positive sign (+) into negative sign (-), and this will led to decrease the value of the critical buckling load (P_{cr}).

3. Experimental Work

3.1. Material used and buckling test machine

AISI 303 stainless steel intermediate and long columns of circular cross-section $D = 8 \text{ mm}, I = 201.1 \text{ mm}^4, r = 2 \text{ mm}$, and different slenderness ratios were tested by using a rotating column buckling test machine which is capable to apply dynamic compression loading (compression-torsion), dynamic bending loading (bending-torsion), and dynamic combined loading (compression-bending and torsion), with column ends support of fixed- pinned and rotating speeds of 17 and 34 r.p.m. In this research, low speed (17 r.p.m) was used in all dynamic buckling experiments (i.e. in both dynamic compression loading and dynamic combined loading). It should be noted that the low speed (17 r.p.m) is chosen in order to give a maximum twisting load because the twisting torque as known is inversely proportional to the rotating speed. Torsion load (twisting moment) has a constant value of $M_t = 280861.7 \text{ N.mm}$ which is corresponding to 0.5 KW of motor power. The photograph of the rotating buckling

test machine is shown in Fig. 2. More details of buckling test machine, used in this research, are in [10]. The detail of the chemical composition of stainless steel is shown in Table 1 and the significant mechanical properties are given in Table 2. Based on the experimental results of the tensile test of 303 AISI stainless steel, the values of tangential modulus (E_t) are calculated for intermediate columns and the results are given in Table 3, and for more details about the method used to determine the values of tangential modulus (E_t) see Appendix A. The geometrical dimensions and buckling parameters of buckling specimens are shown in Table 4.

3.2. Failure criterion of buckling

When the maximum deflection of the column reaches the critical value of deflection (δ_{cr}) of the column length, then the load measured (by pressure gauge, see Appendix B) is the critical buckling load of the column. In the present work, the value of the critical deflection of the column is taken as ($\delta_{cr}(mm) = (L * 1\%) + \delta_o$) [17, 20, and 21]. The initial deflection of the column (δ_o) is measured by using a dial gauge, see Fig. 3. And with a column rotating effect then, the measured value is divided by two (i.e. δ_o = (measured value by dial gauge)/2) to determine the correct value of (δ_o). Because of the rotating effect on the reading of the column deflection using a dial gauge, a laser cell circuit tool was fabricated, with whistle sound, fixed on electronic vernier (with a reading accuracy of 0.01 mm), Fig. 3, to make the reading of critical deflection (δ_{cr}) more strict.

The steps of using a laser cell circuit as a tool for buckling failure criterion can be summarized as follows:

1. Calculation of the magnitude of the lateral critical deflection of the column length in millimeters.
2. Operate the laser-ray circuit and Laser-ray are initially keep tangentially to the surface of the column at the required position (for the present paper: 0.35 of the column length from pinned-end support). This position represents a reference level for the lateral deflection measurement.
3. Input the value of the critical lateral deflection (δ_{cr}) in the digital vernier, this is represented by movement of vernier head and as a resultant changing the level of the laser-ray into a new one that represent the required failure criterion.
4. After exerting of the loads on the column, the column begins to deflect laterally with spiral (deflect) shape, and when the column deflection reaches the critical value (δ_{cr}) then it cross the laser-ray and a whistle warning sound is break out which signify the end of the experiment.

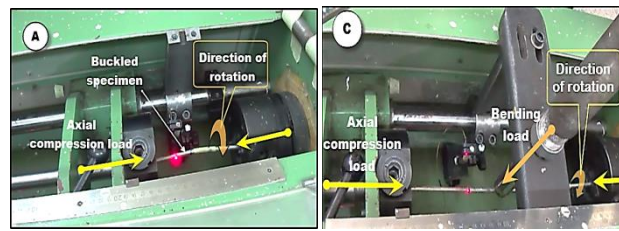Fig. 4 shows some of buckling specimens before and after buckling test.

Figure 2. The rotating buckling test machine and types of loading used in the present research:
(A) dynamic axial compression load, (C) dynamic combined load.

Table 1. Chemical compositions (wt. %) of the used and standard AISI 303 stainless steel

Alloy	C	Si	Mn	P	Cr	Ni
Used material [a]	0.114	0.539	1.14	0.032	18.20	8.19
Standard (ASM) [19]	Up to 0.15	Up to 1.0	Up to 2.0	Up to 0.2	17-19	8-10

[a] Source: State Company for Inspection and Engineering Rehabilitation (SIER)/Baghdad.
Laboratory and Engineering Inspection Department
Minerals Lab. (Spectral analysis of metals) stainless steel rod samp*le*

Table 2. Experimental mechanical properties of AISI 303 stainless steel used in present work
(Average of three specimens)

AISI 303 stainless steel	σ_{ult} (Mpa)	σ_y [a] (Mpa)	E (Gpa)	Elongation[b] %	σ_{pl} (Mpa)
Experimental properties	880	673	204.2	41.4	269.2

[a] Proof stress at 0.2% of stain;   [b] in gauge length $L_o = 25\ mm$

Table 3. Values of Tangential modulus for intermediate columns

No.	L (mm)	L_e (mm)	λ_e $(=\dfrac{L_e}{r})$	E_t (GPa)
1	160	112	56	137.131
2	170	119	59.5	146.248
3	180	126	63	154.764
4	190	133	66.5	162.686
5	200	140	70	170.035
6	210	147	73.5	176.836
7	220	154	77	183.123
8	230	161	80.5	188.928
9	240	168	84	194.288

Table 4. Geometrical dimensions and buckling parameters of the used specimens

No.	Symbol	L (mm)	L_e [a] (mm)	δ_o (mm)	δ_{cr} [b] (mm)	λ_e $(\dfrac{L_e}{r})$	Type of loading	Type [c] of column
1	1a	160	112	0.55/2	1.88	56	dynamic comp.	
	1b			0.9/2	2.05		combined	Intermediate
2	2a	170	119	0.6/2	2	59.5	dynamic comp.	

	2b			1.1/2	2.25		combined	
3	3a	180	126	0.71/2	2.16	63	dynamic comp.	
	3b			1.24/2	2.42		combined	
4	4a	190	133	0.96/2	2.38	66.5	dynamic comp.	
	4b			1.3/2	2.55		combined	
5	5a	200	140	0.8/2	2.4	70	dynamic comp.	
	5b			1.3/2	2.65		combined	
6	6a	210	147	1.22/2	2.71	73.5	dynamic comp.	
	6b			1.46/2	2.83		combined	
7	7a	220	154	1.1/2	2.75	77	dynamic comp.	
	7b			1.6/2	3		combined	
8	8a	230	161	1.21/2	2.91	80.5	dynamic comp.	
	8b			1.4/2	3		combined	
9	9a	240	168	1.2/2	3.0	84	dynamic comp.	
	9b			1.5/2	3.15		combined	
10	10a	260	182	1/2	3.1	91	dynamic comp.	
	10b			1.3/2	3.25		combined	
11	11a	280	196	0.95/2	3.28	98	dynamic comp.	
	11b			1/2	3.3		combined	
12	12a	300	210	1.15/2	3.58	105	dynamic comp.	
	12b			0.95/2	3.48		combined	
13	13a	320	224	1.2/2	3.8	112	dynamic comp.	
	13b			0.8/2	3.6		combined	
14	14a	340	238	1.48/2	4.14	119	dynamic comp.	
	14b			1.1/2	3.95		combined	
15	15a	360	252	1.3/2	4.25	126	dynamic comp.	Long
	15b			1.15/2	4.18		combined	
16	16a	380	266	1.43/2	4.52	133	dynamic comp.	
	16b			1.2/2	4.4		combined	
17	17a	400	280	1.26/2	4.63	140	dynamic comp.	
	17b			0.9/2	4.45		combined	
18	18a	420	294	1.45/2	4.93	147	dynamic comp.	
	18b			1/2	4.7		combined	
19	19a	440	308	1.58/2	5.19	154	dynamic comp.	
	19b			1.3/2	5.05		combined	
20	20a	460	322	1.8/2	5.5	161	dynamic comp.	
	20b			2.3/2	5.75		combined	

[a] $L_e = KL$; [b] $\delta_{cr}(mm) = (L * 1\%) + \delta_o$

[c] $\lambda_c = \pi.\sqrt{\frac{E}{\sigma_{pl}}} = 86.5$, *if* $\lambda_e > \lambda_c \rightarrow long\ column$ and *if* $\lambda_e < \lambda_c \rightarrow intermediate\ column$
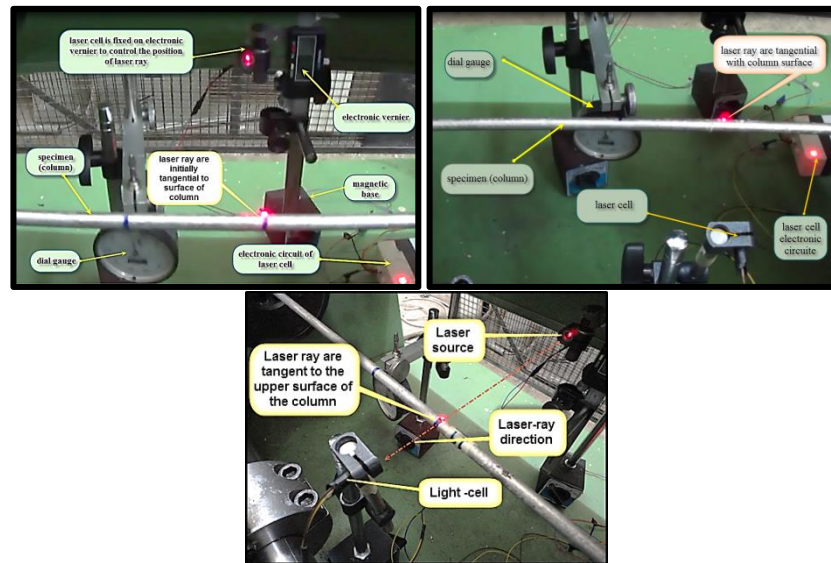
Figure 3. System used to control the deflection of columns during buckling test.

Figure 4. Specimens before and after buckling test.

4. Results and Discussion

Table 5 shows the experimental results of dynamic buckling test of 303 AISI column specimens. In this table, it can be observed that the critical buckling stress (σ_{exp}) decreased with the increase in effective slenderness ratio (λ_e) for both dynamic compression load (compression-torsion load) and dynamic combined load (compression-bending-torsion load). In order to make a comparison between the experimental results and theoretical results, (19) is used to calculate the theoretical critical buckling load (P_{cr}) for the specimens under both dynamic compression load and dynamic combined load, and the results are shown in Table 6 for dynamic compression load and Table 7 for dynamic combined load. From Table 5 and Table 6, it can be observed that there is a good agreement between the experimental critical buckling load (P_{exp}) and the theoretical critical buckling load (P_{cr}) predicts from (19) and the maximum percentage error under dynamic compression load and under dynamic combined load is 19.3% and 16.8%, respectively. Fig. 5 and Fig. 6 are plotted by using the experimental results of Table 5 for specimens under dynamic compression load, whereas Table 6 and Table 7 are gave the theoretical results from derived equation (19). It can be observed that the derived equation (19) may be used to describe the buckling behavior of intermediate and long columns under both dynamic compression load and under dynamic combined load.

The contribution of the torsional loading (twisting moment) in the required critical buckling load is decreased with the increase in the length or slenderness ratios of columns , but this contribution is essentially to determine the accurate theoretical critical buckling load (P_{cr}) form (19) so, the effect of torsional loading can't be neglected. The lateral loading (bending load) on the rotating columns leads to a fast increasing in the lateral deflection of the column under combined loading conditions and a signification reduction in the axial compressive load and as a result, it decreases the critical buckling load of the columns compared with the case without lateral loading (dynamic compression loading) . It is experimentally, noted that the effect of the bending loading in decreasing the critical buckling load was much greater than the effect of the twisting or torsional loading in increasing of the critical buckling load for the same lengths (slenderness ratios) and this fact is provided theoretically by using (19).

Table 5. Experimental results of dynamic buckling test

No.	Symbol	Type of loading	P_{exp} (N)	σ_{exp} (MPa)	$F_{ben.}$ (N)	$\sigma_{ben.}$ (MPa)
1	1a	dynamic comp.	16257.742	323.4375	---	---
	1b	combined	7775.442	154.688	489.6	243.507
2	2a	dynamic comp.	14844.025	295.3125	---	---
	2b	combined	7068.583	140.625	469.2	247.946
3	3a	dynamic comp.	13783.738	274.2188	---	---
	3b	combined	6361.725	126.563	448.8	251.117
4	4a	dynamic comp.	12370.021	246.0938	---	---
	4b	combined	6008.296	119.531	428.4	253.019
5	5a	dynamic comp.	10956.304	217.9688	---	---
	5b	combined	5654.867	112.5	408	253.653
6	6a	dynamic comp.	10249.446	203.9063	---	---
	6b	combined	5301.434	105.469	387.6	253.019
7	7a	dynamic comp.	9542.5877	189.8438	---	---
	7b	combined	4948.008	98.438	367.2	251.117
8	8a	dynamic comp.	9189.1585	182.8125	---	---
	8b	combined	4806.637	95.625	346.8	247.946
9	9a	dynamic comp.	8482.3002	168.75	---	---
	9b	combined	4665.265	92.813	326.4	243.507
10	10a	dynamic comp.	7422.0126	147.6563	---	---
	10b	combined	4523.893	90	306	247.312
11	11a	dynamic comp.	6785.8401	135	---	---
	11b	combined	4241.15	84.375	285.6	248.58
12	12a	dynamic comp.	6008.296	119.5313	---	---
	12b	combined	3887.721	77.3438	265.2	247.312
13	13a	dynamic comp.	5301.4376	105.4688	---	---
	13b	combined	3534.292	70.3125	244.8	243.507
14	14a	dynamic comp.	4948.0084	98.4375	---	---
	14b	combined	3322.234	66.0938	224.4	237.166
15	15a	dynamic comp.	4665.2651	92.8125	---	---

	15b	combined	3180.863	63.2813	204	228.288
16	16a	dynamic comp.	4241.1501	84.375	---	---
	16b	combined	3039.491	60.4688	183.6	216.874
17	17a	dynamic comp.	3887.7209	77.34375	---	---
	17b	combined	2827.433	56.25	163.2	202.923
18	18a	dynamic comp.	3534.2917	70.3125	---	---
	18b	combined	2686.062	53.4375	142.8	186.435
19	19a	dynamic comp.	3180.8626	63.28125	---	---
	19b	combined	2474.004	49.2188	122.4	167.411
20	20a	dynamic comp.	2827.4334	56.25	---	---
	20b	combined	2120.575	42.1875	81.6	116.68

Table 6. Theoretical values of critical buckling load using (19) under dynamic compression load

No.	L (mm)	ℓ (mm)	δ_o (mm)	δ_{cr} (mm)	δ_Q^* (mm)	δ_{max}^* (mm)	H	P_{cr} (N)	P_{exp} (N)	Error %
1	160	10	-0.55/2	-1.88	-1.6	2.183	-12.963	15835.931	16257.742	-2.595
2	170	11	-0.6/2	-2	-1.7	2.335	-13.851	14782.228	14844.025	-0.416
3	180	10	-0.71/2	-2.16	-1.8	2.548	-14.325	13923.073	13783.738	1.011
4	190	10	-0.96/2	-2.38	-1.9	2.902	-15.006	12414.393	12370.022	0.359
5	200	15	-0.8/2	-2.4	-2	2.842	-16.722	11772.94	10956.305	7.454
6	210	10	-1.22/2	-2.71	-2.1	3.368	-16.367	10771.182	10249.447	5.090
7	220	16	-1.1/2	-2.75	-2.2	3.349	-18.291	9973.695	9542.588	4.518
8	230	13	-1.21/2	-2.905	-2.3	3.562	-18.350	9690.538	9189.159	5.456
9	240	14	-1.2/2	-3	-2.4	3.653	-19.238	9263.168	8482.300	9.206
10	260	17	-1/2	-3.1	-2.6	3.654	-21.221	8753.701	7422.013	17.942
11	280	15	-0.95/2	-3.275	-2.8	3.808	-22.168	8094.641	6785.840	19.287
12	300	17	-1.15/2	-3.575	-3	4.213	-23.944	6888.278	6008.296	14.646
13	320	17	-1.3/2	-3.85	-3.2	4.568	-25.306	6099.157	5301.438	15.047
14	340	14	-1.48/2	-4.14	-3.4	4.954	-26.046	5550.473	4948.009	12.176
15	360	13	-1.3/2	-4.25	-3.6	4.975	-27.200	5296.112	4665.265	13.522
16	380	13	-1.43/2	-4.515	-3.8	5.309	-28.769	4754.383	4241.150	12.101
17	400	15	-1.26/2	-4.63	-4	5.341	-30.544	4456.744	3887.721	14.636
18	420	14	-1.45/2	-4.925	-4.2	5.736	-31.906	4034.401	3534.292	14.150
19	440	16	-1.58/2	-5.19	-4.4	6.071	-33.268	3703.398	3180.863	16.427
20	460	18	-1.9/2	-5.55	-4.6	6.597	-35.043	3300.375	2827.433	16.727

Table 7. Theoretical values of critical buckling load using (19) for specimens under dynamic combined load

No.	L (mm)	ℓ (mm)	δ_o (mm)	δ_{cr} (mm)	δ_Q^* (mm)	δ_{max}^* (mm)	H	P_{cr} (N)	P_{exp} (N)	Error %
1	160	15	-0.9/2	-2.05	-1.6	2.536	-13.996	8610.965	7775.442	10.745
2	170	16	-1.1/2	-2.25	-1.7	2.839	-14.884	7748.431	7068.583	9.618
3	180	16	-1.35/2	-2.475	-1.8	3.193	-15.565	7033.603	6361.725	10.561
4	190	16	-1.3/2	-2.55	-1.9	3.245	-16.245	6869.471	6008.296	14.333
5	200	17	-1.3/2	-2.65	-2	3.347	-17.133	6545.262	5654.867	15.745
6	210	16	-1.46/2	-2.83	-2.1	3.609	-17.606	6176.227	5301.438	16.501

| 7 | 220 | 16 | -1.65/2 | -3.025 | -2.2 | 3.903 | -18.287 | 5748.798 | 4948.008 | 16.184 |
8	230	16	-1.6/2	-3.1	-2.3	3.954	-18.968	5614.802	4806.637	16.813
9	240	17	-1.7/2	-3.25	-2.4	4.157	-19.855	5288.082	4665.265	13.350
10	260	15	-1.4/2	-3.3	-2.6	4.058	-20.802	5195.487	4523.893	14.845
11	280	15	-1/2	-3.3	-2.8	3.858	-22.163	4819.482	4241.150	13.636
12	300	14	-0.95/2	-3.475	-3	4.011	-23.317	4260.695	3887.721	9.594
13	320	13	-0.8/2	-3.6	-3.2	4.063	-24.471	3875.768	3534.292	9.662
14	340	11	-1.1/2	-3.95	-3.4	4.569	-25.418	3351.193	3322.234	0.872
15	360	12	-1/2	-4.1	-3.6	4.672	-26.987	3062.323	3180.863	-3.727
16	380	12	-0.98/2	-4.29	-3.8	4.855	-28.348	2836.804	3039.491	-6.668
17	400	10	-0.9/2	-4.45	-4	4.978	-29.295	2734.854	2827.433	-3.274
18	420	11	-1/2	-4.7	-4.2	5.283	-30.863	2568.558	2686.062	-4.375
19	440	11	-1.3/2	-5.05	-4.4	5.789	-32.224	2420.029	2474.004	-2.182
20	460	18	-2.3/2	-5.75	-4.6	7.001	-35.035	2300.938	2120.575	8.505
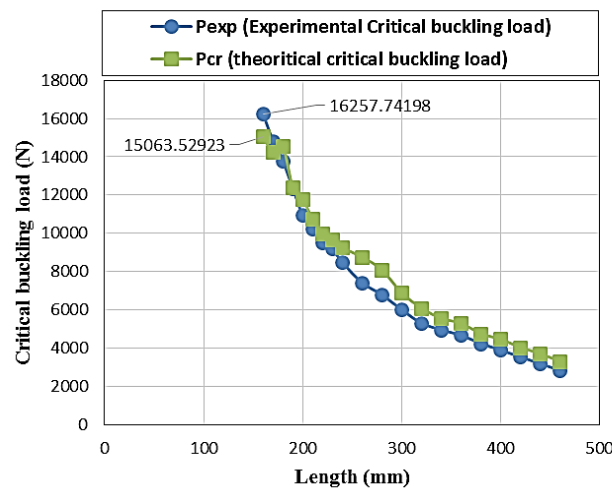
Figure 5. Critical buckling load- length relation for stainless steel 303 AISI columns under dynamic compression loads compared with theoretical buckling load (Eq. 19).
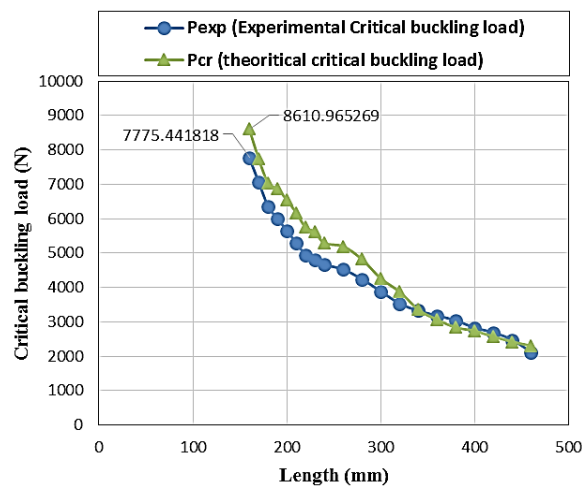

Figure 6. Critical buckling load- length relation for stainless steel 303 AISI columns under dynamic combined loads compared with theoretical buckling load (Eq. 19).

5. Conclusions

1. A new equation has been derived using energy technique (dummy load method) to describe the buckling behavior of intermediate and long columns under dynamic compression load and under dynamic combined load with consider of the initial imperfections of the column and the effect of eccentricity.

2. The theoretical critical buckling load expression
$P_{cr} = \frac{(\delta_Q{}^*)EI}{0.715(\delta_{max}{}^*)HL} - \frac{0.1018M_t}{H} + \frac{8.704427\times10^{-3}FL^2}{0.715(\delta_{max}{}^*)H}$ may be used to predict of the critical buckling load under both dynamic compression and combined load with maximum percentage error is 19.3% and 16.8%, respectively.

3. The derived model (19) is applicable to be applied for other than stainless steel materials because it does not depend on special mechanical properties of column material, and the present model can be re-derived, by using the same previous process, to predict the critical buckling load for other types of column's end conditions.

4. The contribution of the torsional loading (twisting moment) in the critical buckling load is dependent on its direction (i.e. Clockwise or anit-clockwise). A clockwise direction of rotation leads to produce a twisting moment contribute in increasing of the critical buckling load of columns and this will appeared clearly from derivation of (19).

5. The contribution of the torsional loading (twisting moment) in the required critical buckling load is decreased with the increase in the length and/or eccentricity of columns and this contribution is essentially to determine the accurate theoretical critical buckling load (P_{cr}) form (19) so, the effect of torsional loading can't be neglected.

6. The lateral loading (bending load) on the rotating columns leads to a fast increasing in the lateral deflection of the column under combined loading conditions and a signification reduction in the axial compressive load (critical buckling load).

7. Effect of the bending load, in decreasing of the critical buckling load, is increased with the increase of the length and/or eccentricity of columns. The average decreasing in the values of the critical buckling load is -37.92% compared with the values of the critical buckling load without lateral bending load for the same length of the column under dynamic combined load.

Abbreviations

Nomenclature	Definition	Units
A	The cross-sectional area of the column	mm^2
E	Modulus of elasticity.	GPa
E_t	Tangent modulus.	GPa
e	Eccentricity of the column	mm
F, $F_{ben.}$	bending load	N
G	Shear modulus	GPa
H	A variable depending on column's length and overhang distance.	mm

I_z	Moment of inertia of the column cross sectional area about z-axis.	mm^4
J	Polar moment of inertia of the column cross sectional area.	mm^4
K	Effective-length factor = 0.7 for fixed-pinned ends support	dimensionless
L, L_e	Unsupported and effective length of the column	mm
ℓ	Overhang distance (measured experimentally)	mm
M_z	Bending moment at any distance x from point B about z-axis.	N. m
M_t	Twisting moment	N. mm
M_e	Moment due to eccentricity effect	N. mm
N_i	Force exerted on i point, where i=1,2,3,…n.	N
P	Axial compression load	N
P_{cr}, P_{exp}	Theoretical and experimental critical buckling load	N
Q	Dummy load	N
R_B	Reaction force at point B	N
r	Smallest radius of gyration of the column	mm
U	Strain Energy	N. mm
V	Shear force	N
$\sigma_{ult}, \sigma_{pl}$	Ultimate and proportional limit of column's material stress	MPa
σ_y	The yield strength	MPa
σ_{exp}	Experimental critical buckling stress	MPa
$\sigma_{ben.}$	Experimental bending stress	MPa
δ_i	Displacement at point i (under load N_i).	mm
δ_Q, δ_Q^*	Displacement under dummy load Q	mm
$\delta_{max}, \delta_{max}^*$	Maximum deflection	mm
δ_o, δ_{cr}	Initial and critical deflection of the column	mm
v	Deflection at any point x(from deflection curve of the column)	mm
v'	Slope at any point x	rad
θ	Slope at x=0	rad
λ_e, λ_c	Effective and critical slenderness ratio	dimensionless
α	Section modulus for shear effect.	dimensionless

6. References

1. M. L. Gambhir (2009). "*Fundamental of Solid Mechanics* ". PHI learning Private Limited, New Delhi.

2. James M. Gere and Barry J. Goodno (2012). "*Mechanics of Materials*". Brief Edition, Cengage Learning.

3. Roy R. Craig, Jr. ((2011). " *Mechanics of Materials*". 3rd Ed, John Wiley & Sons, Inc.

4. N. R. Baddoo (2003). " *A Comparison of Structural Stainless Steel Design Standards*". the Steel Construction Institute, p.p. 131-149.

5. Ansel C. Ugural, and Saul K. Fenster (2003). "*Advanced Strength and Applied Elasticity*". 4th edition, Prentice-Hall, Inc.

6. V. N. Vazirani, M. M. Raaatwani, and S, K, Duggal (2010). " *Analysis of Structures*". Khanna Publishers.

7. T. H. G. Megson (1999). "*Aircraft Structures for Engineering Students*". 3rd edition, Butterworth-Heinemann.

8. William A. Nash (1998). "*Theory and Problem of Strength of Materials*". Schaum's Outline Series 4th edition, McGraw-Hill, Inc.

9. R. C. Hibbeler, SI conversion by S. C. Fan (2004). " *Statics and Mechanics of Materials*", Prentice-Hall, Inc.

10. Kifah Hameed Al-Jubori (2005). "*Columns Lateral Buckling Under Combined Dynamic Loading*". PhD. Thesis, University of Technology, Department of Technical Education.

11. L. Gardner, D.A. Nethercot (2004). "*Experiments on Stainless Steel Hollow Sections-Part 2: Member Behavior of Columns and Beams*". Journal of Constructional Steel Research, Vol. 60, p.p. 1319-1332.

12. N. Boissonnade, J. P. Jaspart, J. P. Muzeau, and M. Villette (2002). "*Improvement of the Interaction Formulae for Beam Columns in Eurocode 3*". Computers and Structures, Vol. 80, p.p. 2375-2385.

13. Jong-Dar Yau (2007). "*Elastic Stability of I-Columns Subjected to Compressions and bi-Moments*". Journal of the Chinese Institute of Engineers, Vol. 30, No. 4, pp. 569-578.

14. Min Yu, Xiaoxiong Zha, Jianqiao Ye, and Chunyan She (2010). "*A Unified Formulation for Hollow and Solid Concrete-Filled Steel Tube Columns under Axial Compression*". Engineering Structures, Vol. 32, p.p. 1046-1053.

15. J. Dario Aristizabal-Ochoa (2011). "*Stability of columns with Semi-Rigid Connections Including Shear Effects Using Engesser, Haringx and Euler Approaches*". Engineering Structures, Vol. 33, p.p. 868–880.

16. Richard G. Budynas (1999)."*Advanced Strength and Applied Stress Analysis*". 2nd edition, McGraw-Hill, Inc.

17. Zdeněk P. Bažant and Luigi Cipolin (2003). "*Stability of Structures Elastic, Inelastic, Fracture, and Damage theories*". Dover Puplications, Inc.

18. James M. Gere (2004). "*Mechanics of Materials*". 6th Ed, Thomson Learning, Inc.

19. ASM Handbook (1994). "*Surface Engineering*". ASM International, Vol. 5.

20. Hamed Ali Hussein (2010). "*Buckling of Square Columns Under Cycling Loads for Nitriding Steel DIN (CK45, CK67, CK101)*". PhD. Thesis, University of Technology, Department of Mechanical Engineering.

21. Al-Alkhawi H. J. M., Al-Khazraji A. N., and Essam Zuhier Fadhel (2014). "Determination the Optimum Shot Peening Time for Improving the Buckling Behavior of Medium Carbon Steel". Eng. & Tech. Journal, Vol. 32, Part (A), No. 3.

22. Bruce G. Johnston (2006), "Guide to Stability Design Criteria for Metal Structures", Springer-Verlag Berlin Heidelberg.

Appendices

Appendix – A

Calculation of Tangent Modulus (E_t)

At point B as shown in Fig. (1), the elastic modulus is the E_t (tangent modulus) if the stress is increased but E (Young's modulus) if the stress is decreased [7]. The tangent modulus is given by [3, 22]:

$$E_t = \frac{d\sigma}{d\varepsilon} \qquad\qquad (A-1)$$

The critical or Engesser stress may be expressed by means of modification of Euler formula in which E_t replaces E :

$$\sigma_T = \frac{P_{cr}}{A} = \frac{\pi^2 E_t}{(\lambda_e)^2} \qquad\qquad (A-2)$$
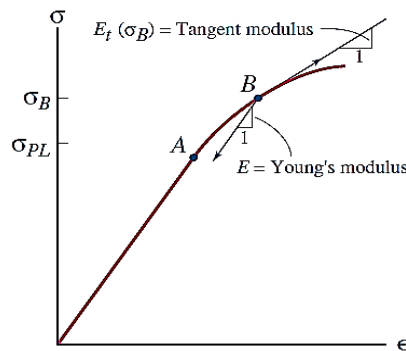
Figure A-1. Stress- strain diagram of a material to illustrate the region of tangent modulus application [22].

From the experimental tensile test results, the stress-strain curve, Fig.2, for 303 AISI stainless steel used in this research can be represented by the following relationship:

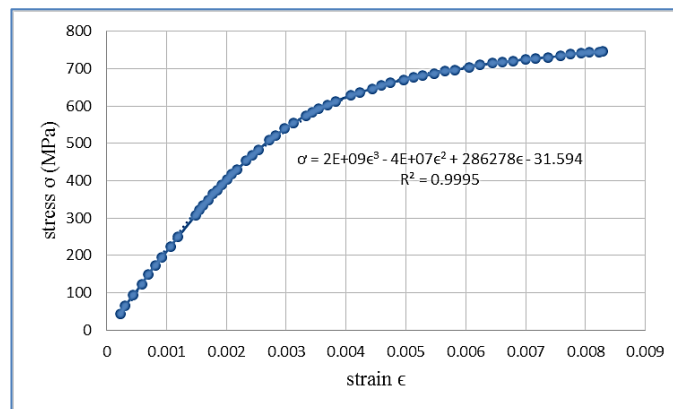$$\sigma = 2*10^9 \varepsilon^3 - 4*10^7 \varepsilon^2 + 286278 \, \varepsilon - 31.594 \qquad\qquad (A-3)$$

Figure (2). Experimental true stress- strain curve of AISI 303 stainless steel used in the present research (as received material)

Where (ε) and (σ) are the uniaxial strain and stress, respectively.
The tangent modulus is given by (A-1):

$$E_t = \frac{d\sigma}{d\varepsilon}$$

So, by differentiation of (A-3) with respect to ε, one can write:

$$E_t = \frac{d\sigma}{d\varepsilon} = 6*10^9\varepsilon^2 - 8*10^7\varepsilon + 286278 \qquad (A-4)$$

Now, substituting (A-3) and (A-4) into (A-2) gives

$$2*10^9\varepsilon^3 - 4*10^7\varepsilon^2 + 286278\,\varepsilon - 31.594$$
$$= \frac{\pi^2}{(\lambda_e)^2} * [6*10^9\varepsilon^2 - 8*10^7\varepsilon + 286278] \qquad (A-5)$$

By rearranging (A-5), one can write:

$$2*10^9\varepsilon^3 - \left(4*10^7 + 6*10^9*\frac{\pi^2}{(\lambda_e)^2}\right)\varepsilon^2 + \left(286278 + 8*10^7*\frac{\pi^2}{(\lambda_e)^2}\right)\varepsilon$$
$$- \left(31.594 + 286278*\frac{\pi^2}{(\lambda_e)^2}\right) = 0 \qquad (A-6)$$

Equation (A-6) can be solved to determine the correct value (root) of real strain ε and then substitute this value in (A-4) to determine the value of the tangent modulus E_t [16].
The following calculations are made for the buckling specimen 1a, see Table 4. This specimens has the following geometrical dimensions: L=160 mm and $\lambda_e = 56$.
From (A-6) and for slenderness ratio λ_e=56

$$2*10^9\varepsilon^3 - \left(4*10^7 + 6*10^9*\frac{\pi^2}{(56)^2}\right)\varepsilon^2 + \left(286278 + 8*10^7*\frac{\pi^2}{(56)^2}\right)\varepsilon$$
$$- \left(31.594 + 286278*\frac{\pi^2}{(56)^2}\right) = 0$$

The above equation is a quadratic equation of 3rd degree so there will be three roots, but one of them will be the true root.
The true root is, $\varepsilon = 2.240986*10^{-3}$
By substituting $\varepsilon = 2.240986*10^{-3}$ in (A-4) this will gives

$$\therefore E_t = 6*10^9*(2.240986*10^{-3})^2 - 8*10^7*(2.240986*10^{-3}) + 286278$$
$$= 137131.238\ MPa = 137.131\ GPa$$

Appendix –B

Calculation of Torsion and Compression Loads
1. Torsion load (twisting moment)

$$Power = \omega * T = \frac{2\pi N * M_t}{60} \qquad (B-1)$$

Where,

Power=driving motor power= 0.5 KW=500 Watt.

ω=angular velocity (rad/sec).

M_t= twisting moment or torque (N.m).

N=rotational speed (r.p.m)= 17 r.p.m (constant)

$$\therefore M_t = \frac{60*Power}{2\pi*N} = \frac{60*500}{2\pi*17} = 280.8617\ N.m = 280861.7\ N.mm$$

2. <u>Axial compression load and compression stress At hydraulic pump</u>

$$p = \frac{F}{A_{cylinder}} \qquad\qquad (B-2)$$

or $\qquad\qquad F = p * A_{cylinder} \qquad (B-3)$

Where,

p: is the applied pressure by hydraulic pump.

F: is the applied load on column.

$A_{cylinder}$: is the cross sectional area of hydraulic pump rod.

<u>At a column</u>

$$\sigma_{comp.} = \frac{F}{A_{column}} \qquad\qquad (B-4)$$

or $\qquad\qquad F = \sigma_{compr.} * A_{column} \qquad (B-5)$

Now, by equating the forces in hydraulic pump and on a column cross sectional area, it can be written

$$\sigma_{compr.} = p * \frac{A_{cylinder}}{A_{column}} = p * \left(\frac{D}{d}\right)^2 \qquad (B-6)$$

Where,

D: is the diameter of hydraulic pump delivery rod.

D=30 mm

d: is the diameter of column.

d= 8 mm (constant for all columns)

$\therefore \sigma_{compr.} = p * (14.0625)$

For a column 1a, Table 5

a recorded pressure $p = 230\ bar = 23\ MPa$, then the compression stress on the column is

$\sigma_{compr.} = \sigma_{exp} = 23 * 14.0625 = 323.438\ MPa$

And the compression load is

$$P_{exp.} = \sigma_{exp} * A_{column} = 323.438 * 10^6 * \frac{\pi}{4}(8)^2 = 16257.742\ N$$